Agricultural and Forest Meteorology 313 (2022) 108763

Contents lists available at ScienceDirect

Agricultural and Forest Meteorology

journal homepage: www.elsevier.com/locate/agrformet

A micrometeorological flux perspective on brush management in a shrub-encroached Sonoran Desert grassland

Enrique R. Vivoni [a,b,*], Eli R. Pérez-Ruiz [a,c], Russell L. Scott [d], Adam T. Naito [e,f], Steven R. Archer [e], Joel A. Biederman [d], Nicole P. Templeton [a]

[a] School of Sustainable Engineering and the Built Environment, Arizona State University, Tempe, AZ 85287, USA
[b] School of Earth and Space Exploration, Arizona State University, Tempe, AZ 85287, USA
[c] Departamento de Ingeniería Civil y Ambiental, Universidad Autónoma de Ciudad Juárez, Ciudad Juárez, México
[d] USDA-ARS Southwest Watershed Research Center, 2000 E. Allen Road, Tucson, AZ 85719, USA
[e] School of Natural Resources and the Environment, University of Arizona, Tucson, AZ 85721, USA
[f] Department of Earth, Environmental and Geographical Sciences, Northern Michigan University, Marquette, MI 49855, USA

ARTICLE INFO

Keywords:
Woody plant encroachment
Brush management
Rangeland
Micrometeorological fluxes
Eddy covariance
Prosopis velutina

ABSTRACT

Woody plant encroachment typically limits the forage productivity of managed rangelands and alters a panoply of semiarid ecosystem processes and services. Intervention strategies to reduce woody plant abundance, collectively termed “brush management”, often lack observations to quantify and interpret changes in ecosystem processes. Furthermore, comparative studies between treated and untreated areas should account for heterogeneity since plant composition, microclimate, topoedaphic factors, and historical land use can substantially vary over short distances in drylands. Here, we quantify ecosystem responses to brush management after a single aerial herbicide application on an 18 hectare shrub-encroached grassland (savanna) in southern Arizona, USA. We conducted a pre- and post-treatment comparison of a flux tower site in the treated area with that of a tower in a nearby control site. The comparison, spanning a seven year period, included: (1) ground, airborne, and satellite-based measurements of vegetation structure, and (2) eddy covariance measurements. The herbicide treatment defoliated the dominant shrub (velvet mesquite, *Prosopis velutina*) and led to a temporary reduction in summer greening, but full foliar recovery occurred within two years. Contrary to expectations, perennial grass cover decreased and bare soil cover increased on the treated site. Relative amounts of evapotranspiration were reduced, while carbon uptake increased during the 2 year post-treatment period at the treated site due to a higher water use efficiency in the following spring. During mesquite recovery, carbon uptake was enhanced by higher gross primary productivity and accompanied by a decrease in ecosystem respiration relative to the untreated site. Mesquite recovery was facilitated by access to deep soil water, carbohydrate reserves in rooting systems, and a lower competition from reduced perennial grass cover.

1. Introduction

Arid and semiarid areas, or drylands, are of global importance as their grasslands, shrublands, and savannas occupy from 40% to 50% of the Earth’s land surface (Sala et al., 2017). Woody plant proliferation in drylands has been widely documented in North America (Huxman et al., 2005; Archer et al., 2017; Schreiner-McGraw et al., 2020), Australia (Noble, 1997), Africa (O’Connor et al., 2014; Venter et al., 2018), and South America (Silva et al., 2001). As a result, encroachment by native or non-native woody plants is a critical management and conservation issue for grasslands and savannas, particularly where the primary land use is livestock grazing (e.g., Naito and Cairns, 2011). In response, intervention strategies in shrub-invaded rangelands have historically focused on reducing woody plants through “brush management” using herbicides, prescribed fire, or mechanical removal (see Scifres, 1980; Hamilton et al., 2004). Brush management effects on herbaceous production range from negative to neutral to positive, are often relatively short-lived and typically require multiple applications for effective management (Archer et al., 2011). Although brush management has been used since the 1960s, its effects on ecosystem processes are

Revised for Agricultural and Forest MeteorologyAGRFORMET-D-21-00596September 24, 2021
* Corresponding author at: School of Earth and Space Exploration, ISTB4, Room 769, Arizona State University, Tempe, AZ 85287-6004, USA.
E-mail address: vivoni@asu.edu (E.R. Vivoni).

https://doi.org/10.1016/j.agrformet.2021.108763
Received 6 May 2021; Received in revised form 24 September 2021; Accepted 1 December 2021

inconsistent and poorly understood (Archer et al., 2011; Archer and Predick, 2014; Ding et al., 2020). This may, in part, reflect that prior work has often assumed that treated and control sites were similar in their function and behavior prior to brush management. However, this assumption is questionable in drylands, where large differences in microclimate, topoedaphic factors, and historical land use can occur over short distances. In this study, we compared ecosystem responses to brush management in an herbicide-treated site to an untreated, control location to explicitly account for pre-treatment differences.

Evaluations of brush management effects have typically used individual plant, small-plot, or transect-based subsampling assessments. Landscape-scale comparisons of treatment effects are less common, especially with respect to ecosystem water, energy, and carbon dioxide (CO_2) exchanges. Since landscapes undergoing woody plant encroachment account for ~30% of global net primary productivity (Field et al., 1998), it is vital to quantify these exchanges with the atmosphere as the herbaceous to woody plant ratio changes (e.g., Dugas et al., 1996; Chen et al., 2003; Williams and Albertson, 2004; Scott et al., 2009, 2015; Verduzco et al., 2015; Morillas et al., 2017; Hinojo-Hinojo et al., 2019). To achieve this, the eddy covariance (EC) method has been widely used to quantify land-atmosphere exchanges (Baldocchi et al., 1988), but its application for brush management studies is limited (e.g., Saleh et al., 2009; Huang et al., 2020). Due to the heterogeneous structure of grass-shrub-tree systems, often a reflection of disturbances associated with livestock grazing, fire, and brush management, EC measurements need to account for differences in plant composition (Detto et al., 2006; Alfieri and Blanken, 2012; Anderson and Vivoni, 2016; Xu et al., 2017; Vivoni et al., 2021). This is important given the varying phenologies and temporal dynamics in landscapes comprised of woody plant patches and interspace areas populated by grasses, herbaceous dicots, succulents or bare soil (Biederman et al., 2018; El-Madany et al., 2018; Schreiner-McGraw and Vivoni, 2018; Ma et al., 2020). Here, we used long-term EC observations, in conjunction with measurements of vegetation structure, to quantify and interpret ecosystem processes in herbicide-treated and control sites.

This study compared multiyear micrometeorological measurements from two EC towers in a semiarid savanna in southern Arizona, USA. While the towers are in close in proximity, their areas presented pre-existing differences in perennial grass, bare ground, and mesquite (*Prosopis velutina*) shrub cover. These differences reflect topoedaphic heterogeneities and variations in grazing, brush management, and fire over many decades. We began by comparing the EC measurements on the two sites over a 4.5 year period. We then conducted an aerial herbicide application that included much of the flux footprint of one tower and then continued monitoring of both towers for an additional 2.5 years. The herbicide used targeted mesquite shrubs and had no known direct physiological effects on grass performance. We complemented the EC measurements with surveys of vegetation characteristics, including cover and height from airborne imagery and ground sampling, phenology from a satellite-based product, and mesquite foliar cover from ocular measurements. Through these measurements, we tracked the spatial and temporal variations in mesquite shrub, grass, and bare soil abundance around both towers. Based on the micrometeorological data and the estimates of the vegetation structure, we address the following questions: (1) "Did the herbicide treatment alter the trajectories of EC fluxes?", (2) "If so, for how long and to what magnitude were water, energy, and carbon fluxes affected?", and (3) "How did changes in the vegetation structure or bare soil cover impact the magnitude and duration of the flux changes?". EC flux perspectives in the context of vegetation structure measurements represent a novel approach for assessing herbicide treatment efficacy and the broad-scale influence of brush management on ecosystem processes and services.

2. Site descriptions and herbicide treatment

The two EC towers are located on the Santa Rita Experimental Range (SRER) in the Sonoran Desert, about 45 km south of Tucson, AZ, on alluvial fans emanating from the Santa Rita Mountains (Fig. 1). The EC towers form part of the AmeriFlux network (sites US-SRM and US-SRS) and were established in 2004 (31.8214°N and 110.8661°W, 1120 m, Scott et al., 2009) and 2011 (31.8173°N and 110.8508°W, 1169 m, Pierini et al., 2014), respectively. Micrometeorological measurements collected from the sites were compared for an overlapping period from January 1, 2012 to December 31, 2018. Both sites were located in the same pasture and experienced low levels of rotational grazing pressure (0.020 to 0.035 animal units yr^{-1} ha^{-1}) for about two winter months each year. Although the sites are in close proximity (~1.5 km), their disturbance histories since the 1970s differed. Mesquite shrubs (*Prosopis velutina* Woot.) in the area surrounding the US-SRS site were treated with a basal application of diesel oil in 1974, recovered one half of their pre-treatment cover by 1986 (Martin and Morton, 1993), and were affected by a wildfire in 1994 (Huang et al., 2007a). In contrast, the US-SRM control site was undisturbed by brush management or fire over this period (Sayre, 2003). Visual observations confirmed that these differences in disturbance histories ostensibly contributed to the sparser cover and lower stature of mesquite and more abundant grass cover at the US-SRS site at the time of herbicide application. For this study, a helicopter herbicide application was conducted on an 18 ha area (Fig. 1c) around US-SRS on June 19, 2016 using a cocktail of clopyralid, aminopyralid, and triclopyr (*Transline, Milestone*, and *Garlon 4 Ultra*; Dow Inc.). Based upon Dow Inc. recommendations, these components were applied at rates of 1157, 512, and 1170 ml ha^{-1}, respectively, and included a surfactant-adjuvant (*Herbimax*; 1170 ml ha^{-1}) to enhance foliar absorption. Dow Inc. guidelines specify that these dicot-specific herbicide components should have little or no direct effect on perennial grass physiology. The aerial application was conducted under low-wind conditions to ensure that herbicide drift was minimized. We saw no evidence of herbicide impacts beyond the directed area of application nor at the 1.5 km distant control site.

Soil surveys at SRER indicated the EC tower sites lie on different series (Breckenfeld and Robinett, 2003). Soils at the US-SRM site are on the Combate-Diaspar complex, with good drainage and sandy loam and loamy sand textures, while the US-SRS site is located on a Sasabe-Baboquivari complex, with less well-drained clay, sandy clay, and sandy clay loam soils. It is important to note that the clayey soils at US-SRS would have intrinsically higher water holding capacities. Soil differences were consistent with the Holocene alluvial deposits at US-SRM, the alluvial fan terrace at US-SRS, and their small elevation difference (US-SRS is 49 m higher). The dominant woody species is velvet mesquite, with subdominants of blue palo verde (*Parkinsonia florida* Benth), catclaw acacia (*Acacia greggii* Gray), and desert hackberry (*Celtis ehrenbergiana* Torr.). Common perennial grasses include the native large-spike bristlegrass (*Setaria macrostachya* Kunth.), Arizona cottontop (*Digitaria californica* Benth), black grama (*Bouteloua eriopoda* Torr.), threeawn (*Aristida* spp.), tanglehead (*Heteropogon contortus* (L.) P Beauv.), and bush muhly (*Muhlenbergia porteri* (Scrib.) Nees.), and the nonnative Lehmann lovegrass (*Eragrostis lehmanniana* Nees.) and Boer/weeping lovegrass (*Eragrostis curvula* (Schad.) Nees.). Perennial forb and annual plant cover were negligible in the pre- and post-treatment periods at both sites. Pre- and post-treatment perennial grass biomass on the US-SRS site was co-dominated by native and non-native grasses, whereas that on the US-SRM site was mainly from native grasses (data not shown). Succulents were present at both sites and included cholla (*Cylindropuntia* spp.), prickly pear (*Opuntia engelmannii* Salm-Dyck), and fishhook barrel cactus (*Ferocactus wislizeni* Britt. & Rose).

The climate of SRER is semiarid (Köppen classification BSh, Beck et al., 2018) with a bimodal precipitation (P) regime and mean annual temperatures of 19 °C. April through June are warm and dry, with mean temperatures that rise towards a maximum in June of 28 °C; high temperatures are sustained during July and August (26 °C), typical of the Sonoran Desert. Summer P (July to September) occurs during the

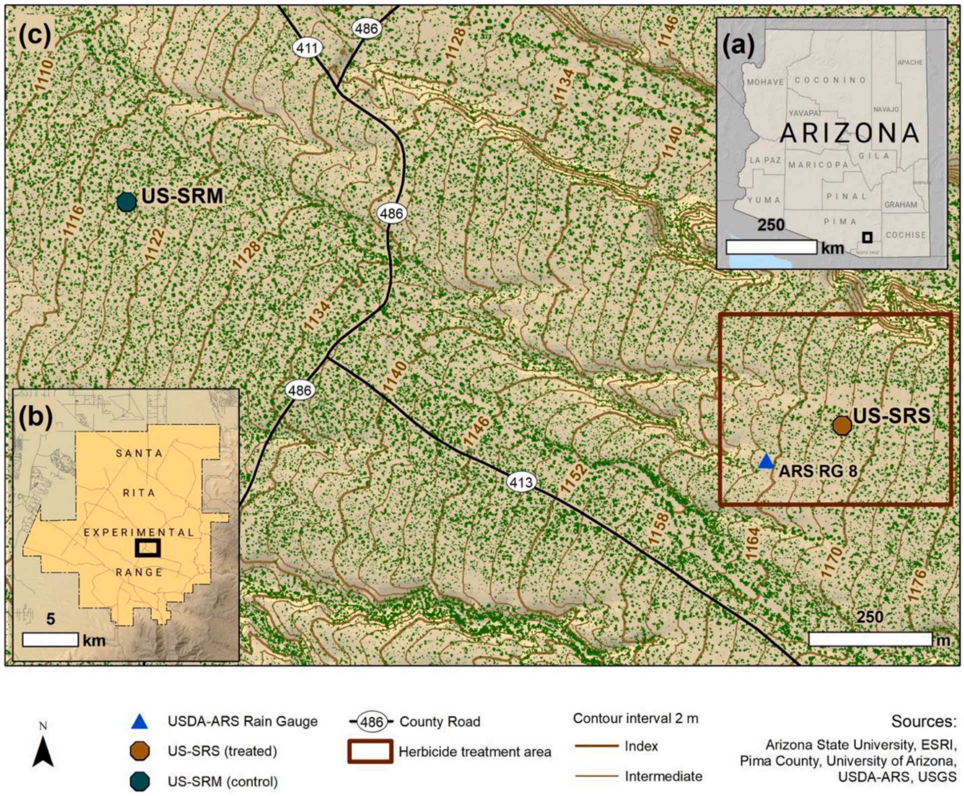

Fig. 1. Location of the study site in (a) Arizona, USA and (b) Santa Rita Experimental Range (SRER). (c) Instrument locations (US-SRM and US-SRS), including the ARS RG 8 rain gage (triangle), relative to the herbicide treatment area, with elevation (m) contours. Representation shows mesquite shrubs in green and bare soil and perennial grass cover as a light brown.

North American monsoon (NAM) (Vivoni et al., 2008), while the cool season (October to March) also has a modest amount of *P*. Precipitation measurements (Fig. 1c) include tipping bucket rain gauges established at each EC tower and longer-term weighing rain gauges maintained by the Agricultural Research Service (ARS). Over the period 1975 to 2008 at ARS Rain Gauge 8 (RG8), the mean annual (calendar year) *P* was 458 mm with 54% occurring during the NAM and 39% during the cool season (Polyakov et al., 2010). Small differences in *P* across sites reflect the localized nature of convective storms during the NAM (Goodrich et al., 2008). Due to the bimodal *P*, there are two green-up periods. The first occurs in spring, with some greening of perennial grasses (early March) and mesquite leaaaf out (early April), the latter species drawing from late fall or winter *P* stored at greater soil depths (Cable, 1977; Scott et al., 2009; Scott and Biederman, 2019). The second green-up occurs during the NAM (mid to late July), when perennial grasses green-up beneath and between mesquite shrubs (Cable, 1975).

3. Methods

3.1. Micrometeorological measurements and data processing

We followed sampling protocols, data processing, and instrument cross-calibration as specified for the AmeriFlux network. Both EC systems consisted of an open path infrared gas analyzer (LI-7500, Li-COR Biosciences, Lincoln, Nebraska) to measure H_2O and CO_2 concentrations and a sonic anemometer (CSAT3, Campbell Sci., Logan, Utah) to measure wind components. Differences included sampling frequency (10 Hz at US-SRM; 20 Hz at US-SRS) and sensor heights and orientations (8 m and 225° at US-SRM, and 7 m and 240° at US-SRS). Processing of the flux measurements into values at 30 min intervals included removal of time periods when: (1) it was raining and the sensors were wet, (2) the wind direction could be obstructed by the tower (±10° from the opposite direction), (3) the friction velocity was less than a threshold (0.19 m s^{-1}), and (4) for outliers > 3 standard deviations (Schmid et al., 2000; Scott et al., 2009). Standard corrections were applied using protocols in Scott et al. (2009). We gap-filled evapotranspiration (*ET*) and daytime net ecosystem exchange (*NEE*) data using look-up tables of *ET, NEE*, and incoming solar radiation for 15 day (*ET*) and 5 day (*NEE*) moving windows separated into periods before and after 12 p.m. (Falge et al., 2001). Missing nighttime *NEE*, assumed equal to ecosystem respiration (R_{eco}), was filled in over the 5 day moving window using a relation with air temperature (Reichstein et al., 2005). This nighttime R_{eco} model was also used to obtain daytime R_{eco}. Gross primary productivity (*GPP*) was then calculated as $GPP = R_{eco} - NEE$, with $NEE < 0$ indicating net CO_2 uptake and $NEE > 0$ representing net CO_2 releases.

Meteorological measurements from each site included: (1) precipitation (*P*), (2) air temperature (T_{air}), (3) relative humidity (*RH*), (4) incoming solar radiation (R_s), and (5) net radiation (R_n), as described in Scott et al. (2009) and Pierini et al. (2014) for US-SRM and US-SRS, respectively. Vapor pressure deficit (*VPD*) was calculated using T_{air} and *RH*. Ground heat flux (*G*) was measured using heat flux plates (5 cm depth), with 0–5 cm heat storage corrections applied using soil thermocouples at 2 and 4 cm depths and soil moisture at 5 cm depth (Scott et al., 2009; Pierini et al., 2014). Available energy, computed as $R_n - G$, was compared to the turbulent fluxes, namely sensible heat flux (*H*) and latent heat flux (λET). We inspected the energy balance closure ($\varepsilon = \sum(H + \lambda ET) / \sum(R_n - G)$) for periods of simultaneously available fluxes (88% and 57% of study period at US-SRM and US-SRS, respectively). For these periods, we found that 87% and 86% of the available energy consisted of turbulent fluxes for US-SRM and US-SRS, within the range reported in other studies (Wilson et al., 2002). Despite the closure shortfall, multi-year (2004–2016) sums of *ET* agreed well (within 3%) with the site water balance at US-SRM (Scott and Biederman, 2019). Using a two-dimensional footprint model (Kljun et al., 2015), we obtained estimates of the multi-year (2015 to 2017) integrated flux source region for each EC tower. Here, we used the 80% contour line, a common metric for the predominant source area (Chu et al., 2021), resulting in footprints of 3.4 ha (US-SRM) and 4.4 ha (US-SRS).

3.2. Ground-based and remotely-sensed vegetation datasets

We generated two circular areas centered on each tower (radii of 60 m and 200 m) for ground sampling and remote sensing image analyses. Vegetation transects ($n = 8$) consisted of 60 m lines extending along the four cardinal and four intermediate compass directions. Along each transect, we recorded grass species and grass, shrub, and bare ground intercepts. Sampling at the US-SRM site was conducted in July 2014 and Septembers of 2017, 2018, and 2019; US-SRS transects were surveyed in November 2015 and Septembers of 2016, 2017, 2018, and 2019. To determine herbicide treatment impacts, we made seasonal ocular estimates of live foliar cover on individual mesquite shrubs (leaf-out in March, at mid-NAM cover in August, at peak cover in September/October) from 2016 through 2019. This was done on shrubs on the treated US-SRS site ($n = 52$) and in an untreated area ($n = 30$), ~200 m to the south of the US-SRS tower.

Ground sampling was supplemented and spatially expanded with remotely-sensed products. Prior to the herbicide application, an April 2011 Light Detection And Ranging (LiDAR) airborne flight provided a 1 m canopy height model (Pima, 2011). USDA National Agriculture Imagery Program (NAIP) airborne orthophotos (0.6 m and 1 m resolution) acquired between June and July in 2013 and 2015 (pre-treatment) and 2017 and 2019 (post-treatment) were classified based on their red, green, and blue signatures at a common resolution of 1 m. Three ground cover classes (mesquite, grass, and bare soil) were quantified after conducting an iterative self-organizing data analysis (ISODATA) unsupervised classification with a maximum of 20 classes and 20 iterations. We validated the classifications using field observations from the transect-based ground sampling described previously. We also used a satellite-based Enhanced Vegetation Index (*EVI*) from the MODerate resolution Imaging Spectroradiometer (MODIS) composites at 250 m and 16 day resolution (ClimateEngine.org, Huntington et al., 2017) centered on the tower sites. This product was preferred over Landsat owing to its ability to account for cloud cover using 16-day compositing (e.g., Mendez-Barroso et al., 2009). Spatially-aggregated *EVI* values were obtained for the 80% source area around each tower and compared for pre- and post-treatment periods. Since the treatment area at US-SRS fully covered the EC footprint and the MODIS pixels used, *EVI* values are expected to reflect the ecosystem response.

4. Results

4.1. Vegetation cover differences and treatment effects

Vegetation and bare soil cover in the areas surrounding each EC tower are shown in Fig. 2 for selected years during pre- (2015) and post-treatment (2017) periods, along with the outlines of the 60 m and 200 m circular areas and 80% source area footprints. Table 1 provides cover data derived from ground transects and remotely-sensed images for all available time periods. During the pre-treatment period, mesquite cover was higher than after one year in the post-treatment period along transects on both sites. This decline along transects at US-SRM could not have been due to the herbicide application. This is an example of the importance of having a pre-treatment perspective on both treated and control sites. On average, NAIP assessments of mesquite shrub cover were lower (~6%) than that of transect-based estimates. When averaged across all measurement scales and dates, pre-treatment mesquite cover on the US-SRM site (27.9%) was higher than that on US-SRS (18.5%). Mesquite shrubs on the US-SRM site were also taller than those at the US-SRS site (e.g., 3.6 ± 3.2 m versus 2.4 ± 2.6 m within the 200 m circular areas) presumably reflecting the higher clay content of the US-

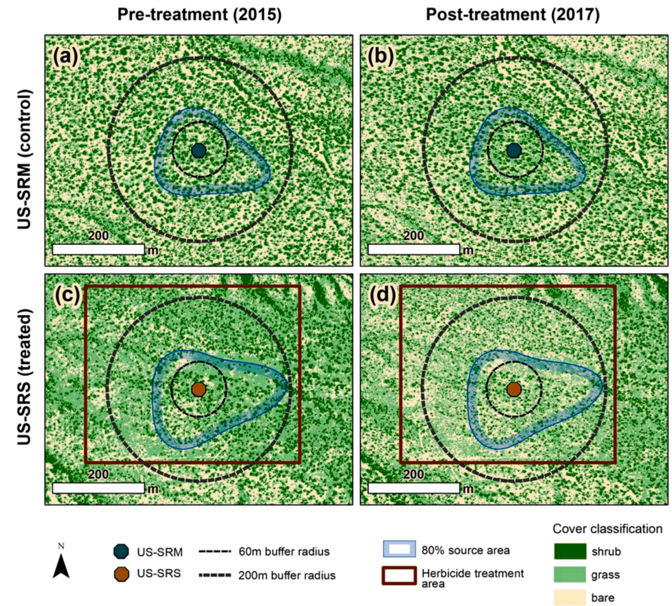

Fig. 2. Vegetation classification from NAIP imagery at the US-SRM (a and b) and US-SRS (c and d) sites on a pre-treatment date (July 2015) and in June 2017, one year after a June 2016 herbicide application on the US-SRS site. Vegetation and bare ground cover in sampling areas centered on EC towers (60 m and 200 m radii and the 80% source area) are summarized in Table 1.

SRS soils and the 1994 wildfire that impacted the US-SRS site, but not the US-SRM site. Grass and bare soil cover were temporally dynamic on both sites. NAIP-based grass cover estimates were consistently higher than the transect-based cover estimates. Pre-treatment NAIP grass cover on the US-SRM (40.9%, averaged across scales) was lower than that on the US-SRS site (59.5%) reflecting the more substantial and diversified grass community on the latter. NAIP-based estimates of bare ground (28.9% averaged across scales) were 16 to 24% lower (absolute) than transect estimates (mean of 49.4%). Pre-treatment NAIP bare ground on the US-SRM site (28.9%, averaged across scales) was comparable to that on the US-SRS site (30.1%).

The herbicide treatment at the US-SRS site minimally affected mesquite shrubs (<7% mortality based on visual inspections that included examination of the cambium near ground level). This mortality had a modest effect on mesquite cover at US-SRS relative to the US-SRM site where no discernable changes in mesquite cover occurred (Table 1). Mesquite foliar cover decreased to 14.6% within the two months following the June 2016 herbicide application (Table 2). Kruskal-Wallis chi square tests indicated statistically significant differences existed between mesquite foliar cover on the treated and untreated areas between August 2016 and March 2018. However, by August 2018, mesquite foliar cover was comparable on treated and untreated plants (67.8 and 67.5%, respectively). Mesquite cover from NAIP estimates within the 200 m circular area surrounding the US-SRS site decreased by 8.5% and 2.9% (absolute) for 2017 and 2019 (1 year and 3 years after treatment, respectively), whereas mesquite shrub cover change at the US-SRM site was −0.8% and +1% over the same periods. Similar results were obtained for the 60 m and 80% source areas and transect-based assessments. Herbicide-induced reductions in mesquite cover were accompanied by an increase in bare soil at the US-SRS site (+19.8% and +18.1% within the 200 m area in 2017 and 2019, respectively), whereas changes at the US-SRM site were minimal (<5%) during this time. Paralleling the increases in bare soil and the recovery of mesquite shrub canopies at the US-SRS site was a decline in grass cover (from 58.8% in 2015 to 48.5% and 44.5% in 2017 and 2019 within the 200 m area, respectively). This was unexpected given that brush management treatments conducted at this site in 1974 generated increases in grass

Table 1
Mean (±1 standard deviation, $n = 8$ transects) cover (%) of mesquite shrubs, grasses, and bare soil at US-SRM and US-SRS sites, and NAIP classifications within 60 m and 200 m of the towers and the 80% source area. Dates for the pre-treatment transect recordings varied (2014 at US-SRM and 2015 at US-SRS). NAIP images were obtained between June 8 and July 2 for 2013 and 2015 (pre-treatment) and 2017 and 2019 (post-treatment).

Area and Year	Herbicide Application	US-SRM (control) Mesquite Cover	Grass Cover	Bare Soil Cover	US-SRS (treated) Mesquite Cover	Grass Cover	Bare Soil Cover
Ground Transects							
2014/5	Pre-treatment	35.9 ± 8.2	14.3 ± 4.2	49.9 ± 7.7	21.3 ± 13.4	46.8 ± 14.0	32.0 ± 12.2
2017	Post-treatment	24.5 ± 10.5	20.0 ± 7.8	55.5 ± 3.7	15.6 ± 7.3	43.8 ± 8.9	40.6 ± 10.9
2018	Post-treatment	23.6 ± 11.3	58.8 ± 13.5	20.6 ± 10.5	14.0 ± 10.0	63.1 ± 20.1	22.9 ± 13.6
2019	Post-treatment	24.2 ± 9.8	31.7 ± 10.4	44.1 ± 13.5	19.9 ± 8.5	57.4 ± 8.6	22.7 ± 10.6
NAIP Imagery 60 m area							
2013	Pre-treatment	23.4	33.9	42.5	14.9	39.8	45.2
2015	Pre-treatment	31.1	43.4	25.0	24.4	58.8	16.6
2017	Post-treatment	30.4	47.4	22.0	14.8	47.7	37.3
2019	Post-treatment	32.0	46.1	21.7	20.3	41.4	38.1
200 m area							
2013	Pre-treatment	23.0	33.2	43.8	13.5	50.0	36.5
2015	Pre-treatment	29.3	37.1	33.6	21.6	59.8	18.6
2017	Post-treatment	28.5	38.9	32.6	13.1	48.5	38.4
2019	Post-treatment	30.3	41.0	28.7	18.7	44.5	36.7
80% source area							
2013	Pre-treatment	22.6	37.9	39.5	13.1	42.7	44.2
2015	Pre-treatment	29.7	42.3	28.0	21.0	59.8	19.2
2017	Post-treatment	29.1	45.8	25.2	12.7	47.8	39.5
2019	Post-treatment	30.6	47.7	21.7	18.2	42.0	39.9

Table 2
Mean (±1 standard deviation) foliar cover (%) of mesquite shrubs (ocular measurements on n individual plants) on the treated site (US-SRS) and a nearby untreated site during post-treatment periods. Bold indicates statistically significant differences ($p < 0.001$) from Kruskal-Wallis chi square tests.

Year	Month	Foliar Cover (%) Untreated site, $n = 30$	US-SRS treated site, $n = 52$
2016	August	64.3 ± 17.9	14.6 ± 10.4
	October	66.6 ± 12.9	22.5 ± 18.6
2017	March	52.7 ± 26.7	28.5 ± 16.1
	August	73.8 ± 16.2	55.7 ± 12.3
	October	67.0 ± 22.8	48.9 ± 14.6
2018	March	61.4 ± 20.6	36.5 ± 20.2
	August	67.5 ± 17.8	67.8 ± 14.7
	October	69.7 ± 10.6	65.4 ± 11.3
2019	September	68.0 ± 19.0	66.9 ± 13.8

cover (Martin and Morton, 1993). Consistent with pre-treatment site differences, grass cover remained lower on the US-SRM site (31.7% and 41.0% in 2017 and 2019) and, like bare soil cover, changed little (<3%) between 2015 and 2019.

We placed the herbicide treatment effects on vegetation into a higher temporal resolution context by computing MODIS-based *EVI* within the 80% source areas for each site (Fig. 3). The seasonality in *EVI* was similar at US-SRM and US-SRS during both pre- and post-treatment periods (separated by vertical dashed line). Throughout the record, the greater mesquite shrub cover and height at the US-SRM site contributed to higher peak summer *EVI*s. During certain years with above-average fall and winter *P* (e.g., 2012, 2016, and 2017), mesquite shrubs on the US-SRM site also exhibited an earlier and more robust spring green-up than those on the US-SRS site. The herbicide effect is noted only at the US-SRS site in Fig. 3b (arrow) where a short-term reduction (~0.5 units) and a temporal delay (~1 month) in *EVI* occurs relative to the summer green-up at the US-SRM site. This behavior was inconsistent with the nearly identical timing of summer green-up occurring for other years in the record. As a result, the treatment impacted mesquite shrub phenology at US-SRS prior to the NAM. Whereas mesquites in the Sonoran Desert typically leaf-off in autumn (van Leeuwen et al., 2010) after grass production has peaked and when grasses are quiescent, the herbicide-induced early leaf-off in June occurred just prior to the onset of the summer rains and allowed for an herbaceous green-up that led to a rapid recovery in *EVI* during the NAM. The modest reduction in *EVI* was

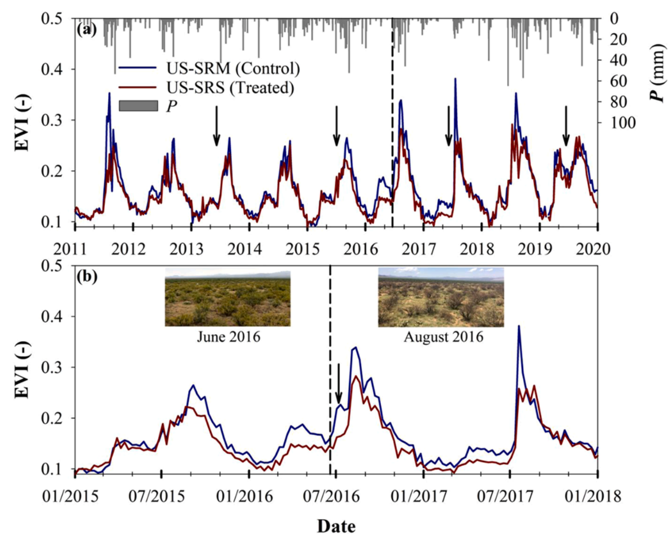

Fig. 3. Daily and seasonal variations in the MODIS Enhanced Vegetation Index (*EVI*) values within the 80% source areas around US-SRM and US-SRS sites for (a) the entire study period and (b) prior to and after the herbicide application. Vertical dashed lines depict the treatment date (June 19, 2016). Daily precipitation (*P*) at the US-SRM site is shown in (a) along with arrows that indicate dates of NAIP imagery (Table 1). Landscape photographs immediately prior to and ~2 months after herbicide application are shown as insets in (b). Arrow in (b) indicates initial mesquite defoliation effect on *EVI*.

coincident with ground-level observations of declines in mesquite foliar cover (Fig. 3 insets).

4.2. Comparisons of meteorological variables for pre- and post-treatment periods

Seasonal cycles of *P*, R_n, T_a, and *VPD* during pre- and post-treatment periods on the two sites are shown in Fig. 4. Consistent with long-term records, the site experienced bimodal *P*, with higher *P* during the NAM (59% of annual total over study period for both sites). Mann-Whitney Rank Sum tests ($p < 0.05$) were performed to compare the distribution of ranks in the pre- and post-treatment groups (Table 3).

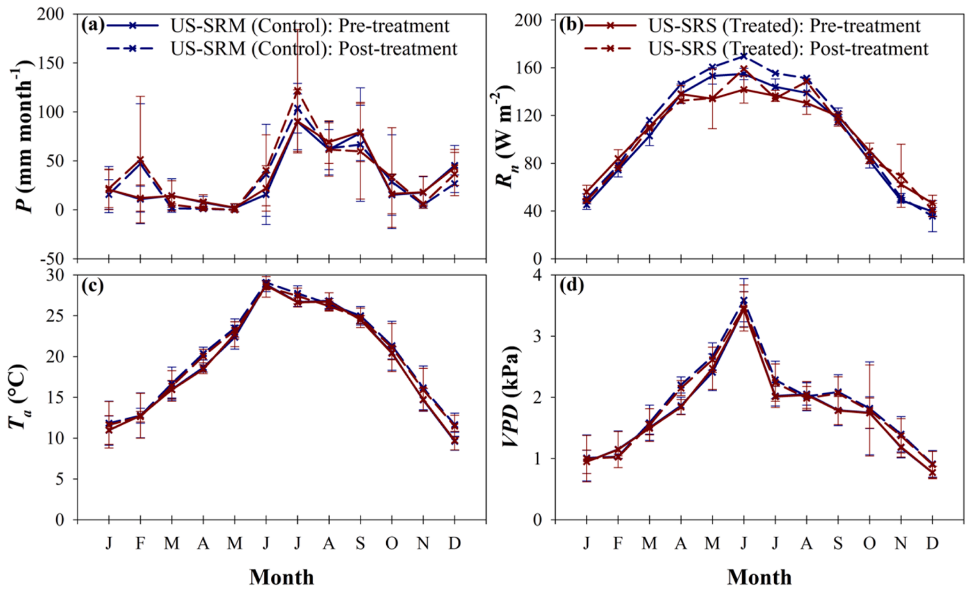

Fig. 4. Monthly meteorological variables at US-SRM and US-SRS sites: (a) total precipitation (P, mm month^{-1}), (b) average net radiation (R_n, W m^{-2}), (c) average air temperature (T_a, °C), and (d) average vapor pressure deficit (VPD, kPa) for pre-treatment (2012–2016) and post-treatment (2016–2018) periods, excluding June 2016. Bars represent ±1 monthly standard deviation. Table 3 presents statistical summaries.

Table 3
Mean (±1 standard deviation) seasonal and annual comparison for pre- and post-treatment periods at US-SRM and US-SRS for precipitation (P, mm), net radiation (R_n, W m^{-2}), air temperature (T_a, °C), vapor pressure deficit (VPD, kPa), and the MODIS Enhanced Vegetation Index (EVI). Data for AMJ in 2016 is omitted since it spans the herbicide application date. Bold indicates significant differences between pre- and post-treatment values within each site; italics indicate significant differences between US-SRM and US-SRS (Mann-Whitney Rank Sum Tests; $p < 0.05$). Seasons denoted as JFM (January – March), AMJ (April – June), JAS (July – September), and OND (October – December). Rank distribution tests of the median, 25%, and 75% quartiles are applied to pre- and post-treatment groups since these have different samples sizes (N_{pre} = 1461 days, N_{post} = 730 days) and failed the Shapiro-Wilk Normality Test.

Site	JFM		AMJ		JAS		OND		Annual	
	Pre-	Post-	Pre-	Post-	Pre-	Post-	Pre-	Post-	Pre-	Post-
US-SRM (control)										
P	46±15	65±45	29±34	37±50	219±23	234±61	*72±21*	61±57	*365±77*	403±252
R_n	*75±4*	80±4	*149±7*	*159±1*	134±6	*148±6*	*59±3*	60±5	104±4	111±2
T_a	13.3 ± 1.3	13.8 ± 0.1	23.5 ± 0.8	24.3 ± 0.3	25.9 ± 0.2	26.4 ± 0.4	15.2 ± 0.7	16.4 ± 2.3	19.4 ± 0.3	20.2 ± 0.7
VPD	1.2 ± 0.1	1.2 ± 0.0	2.6 ± 0.2	2.8 ± 0.0	1.9 ± 0.1	2.1 ± 0.1	1.2 ± 0.1	1.4 ± 0.4	1.7 ± 0.1	1.9 ± 0.2
EVI	0.12±0	*0.11±0*	*0.15±0*	*0.14±0*	*0.21±0*	*0.25±0*	0.15±0.1	0.17±0	0.15±0	0.17±0
US-SRS (treated)										
P	48±13	79±44	31±35	38±48	237±29	244±15	*71±17*	76±54	*387±30*	431±175
R_n	*84±1*	78±0	*138±10*	*142±0*	130±6	*125±10*	*67±4*	65±6	106±2	108±0
T_a	13.2 ± 1.3	13.6 ± 0.1	23.4 ± 0.8	23.9 ± 0.2	25.8 ± 0.2	26.1 ± 0.4	15.2 ± 0.7	16.2 ± 2.2	19.4 ± 0.3	20.0 ± 0.6
VPD	1.2 ± 0.1	1.2 ± 0.0	2.6 ± 0.2	2.7 ± 0.4	1.9 ± 0.1	2.1 ± 0.0	1.2 ± 0.1	1.4 ± 0.4	1.7 ± 0.1	1.9 ± 0.1
EVI	0.12±0	*0.11±0*	*0.14±0*	*0.13±0*	*0.20±0*	*0.22±0*	0.14±0	0.16±0	0.15±0	0.16±0

Tests indicated significant pre-treatment differences in P existed between US-SRM and US-SRS at the annual scale and for the period of October to December (OND). However, P was comparable during the post-treatment period, indicating that any site differences in turbulent fluxes after the herbicide application cannot be attributed to differences in P. Similarly, T_a and VPD exhibited no significant differences between US-SRM and US-SRS for either the pre- or post-treatment periods in any season or over the annual scale. Interestingly, significant site differences were noted in R_n for different seasons in opposing directions, leading to similar annual values (Table 3). These dynamics were associated with differences in vegetation phenology around each tower. The higher EVI at the US-SRM site during the warm season (April-September, Table 3) led to higher R_n, whereas lower grass cover at US-SRM during the cool season (October-March, Table 1) reduced R_n, relative to the US-SRS site.

Herbicide impacts were assessed through comparisons of pre- and post-treatment periods (Table 3). Significant differences in P among periods occurred in particular seasons, but annual totals were similar. Of note were the significantly higher P for JFM within the US-SRS site after the treatment, with a similar behavior between pre- and post-treatment periods at US-SRM for AMJ. T_a and VPD differed significantly between the pre- and post-treatment periods at both EC towers. Because this occurred at both sites, we attribute it to meteorological differences between the periods, not treatment effects. Similarly, significant differences were noted in R_n between pre- and post-treatment periods at both sites, with more marked changes at the US-SRM site. This suggests increases in R_n at the control site are due to meteorological variations, as reflected in P, T_a, and VPD (Table 3), since there were no herbicide treatment effects *per se* at US-SRM. It is important to note that opposing changes occurred in R_n at the US-SRS site, with significant decreases during the cool season (October-March) and no significant changes during the warm season (April-September). This apparent treatment effect was large enough to overwhelm the influence of meteorological variations that occurred between the two periods at the US-SRM site. We attributed this treatment effect to decreases in both mesquite and grass cover at US-SRS (see, for instance, Table 1, 60 m area from 2015 to 2017).

4.3. Treatment effects on water, energy, and carbon fluxes

Interannual comparisons of the micrometeorological fluxes are presented in Table 4 for pre- and post-treatment periods. Mean annual *P* over 2012–2018 showed a small difference between the sites (382 and 407 mm yr^{-1} at US-SRM and US-SRS sites, respectively) that were within the interannual standard deviations (118 and 79 mm yr^{-1}). The post-treatment period consisted of the driest (2017) and wettest (2018) years in the study record at both sites. These differences in *P* were reflected in large interannual differences in *ET, GPP*, and R_{eco}, with the US-SRM site having larger coefficient of variations (CVs) for all variables. Note that two years with higher *P* at USR-SRM, due to the effects of single storms, had a considerable effect on the site differences in *ET, GPP*, and R_{eco} (Table 4). The slight, but consistently higher *P* at the US-SRS site, along with differences in vegetation composition, resulted in a slightly greater mean annual *ET*, a lower *ET/P* (interannual mean *ET/P* of 0.94 and 1.00 at US-SRM and US-SRS, respectively), and a substantially greater *GPP* and R_{eco}. This provides an initial indication that the US-SRS site was more productive during the entire pre- and post-treatment periods, with an interannual mean *NEE* of −165 g C m^{-2} yr^{-1} as compared to −20 g C m^{-2} yr^{-1} at the US-SRM site. *NEE* averaged over the pre-treatment period was −23 and −133 g C m^{-2} yr^{-1} on the US-SRM and US-SRS sites, respectively. We attribute the higher productivity at US-SRS during the pre-treatment period to the higher *P* and a greater soil water holding capacity promoting more extensive grass cover. These values shifted to −99 and −199 g C m^{-2} yr^{-1} at the US-SRM and US-SRS sites during the treatment year of 2016, and subsequently to +25 and −213 g C m^{-2} yr^{-1} when averaged over the two years in the post-treatment period, in response to vegetation changes.

Seasonal cycles of the surface energy balance (R_n – *G, H*, and λET) and carbon fluxes (*NEE, GPP*, and R_{eco}) are shown in Fig. 5 for pre- and post-treatment periods and statistically significant differences using the Mann-Whitney Rank Sum tests ($p < 0.05$) are shown in Table 5. As discussed previously, R_n decreased after the herbicide treatment due to vegetation and bare soil cover changes at US-SRS. Significantly larger λET values were typically noted at the US-SRS site, except for July to September in the post-treatment period when a reversal occurred (71 and 67 W m^{-2} at US-SRM and US-SRS, respectively). US-SRS exhibited a lower *H* for most seasons and both periods, but site differences were not significant. After the herbicide application, a reversal in the relative magnitude of *H* at the sites occurred in July to September (Table 5), closely linked to λET changes. Note that there were significant site differences in *NEE, GPP*, and R_{eco} that are attributable to the herbicide treatment effect at US-SRS. US-SRS had larger *GPP* and R_{eco} values than US-SRM throughout the year for both pre- and post-treatment periods and a consistently negative *NEE*, leading to net uptake in two seasons: early March to June, and late July to October. In contrast, the US-SRM site exhibited weakly negative or slightly positive *NEE*, suggesting near carbon neutrality (Table 5). After the treatment, US-SRS had a significantly lower *NEE* (more CO_2 fixation), relative to the pre-treatment difference with US-SRM, throughout most of the year, primarily due to significant reductions in R_{eco}.

The impact of the herbicide treatment on four indices, *ET/P* ratio, water use efficiency (*GPP/ET*), R_{eco}/GPP ratio, and R_{eco}/P ratio are summarized in Fig. 6. The indices were pooled to represent the six month periods before and after the NAM onset: Dry (January – June) and Wet (July – December). Note that *ET/P* was typically >1 during the Dry periods, and <1 for the Wet seasons at both EC towers. Prior to the treatment, US-SRS consistently had higher *ET/P*, whereas a reversal occurred after the herbicide application. *GPP/ET* was also consistently greater at US-SRS prior to the treatment, but within the range of values that have been reported across a wider number of sites in the region (Biederman et al., 2016). The water use efficiency at US-SRS, however, was reduced relative to the US-SRM site in the first Wet season after mesquite defoliation and grass cover loss, resulting in similar *GPP/ET* at both sites. This impact was limited to a single season as a large rebound in *GPP/ET* occurred at US-SRS for the subsequent Dry season. This dynamic was not evident at US-SRM, where instead, a larger amount of R_{eco} occurred, as shown by the high value of R_{eco}/GPP. The relative value of R_{eco}/GPP decreased at US-SRS after the treatment, indicating a more efficient capture of CO_2 (Biederman et al., 2018). The R_{eco}/P ratio revealed that the herbicide application temporarily shifted the behavior of the two sites. Prior to the treatment, R_{eco}/P was greater at US-SRS than at the US-SRM site, but a reversal was noted after the herbicide application, coincident with relative changes in *ET/P*.

5. Discussion

5.1. Vegetation cover variations

Mesquite shrub cover was greater at the US-SRM control site than the US-SRS treated site prior to and after the herbicide treatment as determined by both ground-based sampling and remote sensing classifications. Overall, mesquite shrubs were also taller at US-SRM as obtained from the LiDAR canopy height model. These differences ostensibly reflect variations in soil conditions (Browning et al., 2008). Specifically,

Table 4
Interannual comparison of the US-SRM and US-SRS sites for precipitation (*P*), net radiation (R_n), evapotranspiration (*ET*), gross primary productivity (*GPP*), and ecosystem respiration (R_{eco}). Average differences (US-SRS minus US-SRM) for pre- and post-treatment periods are labeled 'Diff'. Interannual statistics are for the entire 2012–2018 period. Dash (-) indicates incomplete data and are excluded from the interannual mean, standard deviation (Std.), and coefficient of variation (CV) comparisons.

Year	*P* (mm)		R_n (W m^{-2})		*ET* (mm)		*GPP* (g C m^{-2})		R_{eco} (g C m^{-2})	
	US-SRM	US-SRS	US-SRM	US-SRS	US-SRM	US-SRS	US-SRM	US-SRS	US-SRM	US-SRS
Pre-Treatment										
2012	307.1	378.9	103.8	104.2	334.8	428.7	374.8	693.9	336.9	529.5
2013	318.3	357.8	98.8	105.0	294.0	414.4	299.6	593.5	311.3	497.1
2014	359.4	382.6	104.7	109.4	307.9	377.1	361.3	571.3	332.0	476.8
2015	474.5	429.2	108.2	104.4	408.9	425.1	458.9	693.5	422.8	516.8
Diff		22.3		1.9		74.9		264.4		154.3
Treatment Year										
2016	406.9	436.4	112.0	–	424.1	430.3	557.2	715.9	458.6	516.5
Diff		29.5		–		6.2		158.7		57.9
Post-Treatment										
2017	224.8	306.8	109.4	108.0	263.4	337.0	236.5	598.7	362.2	451.9
2018	581.6	554.5	112.0	–	469.9	446.8	569.2	771.4	494.2	491.7
Diff		27.5		–		25.3		282.2		43.6
Interannual Statistics										
Mean	381.8	406.6	107.0	106.2	357.5	408.5	408.2	662.6	388.3	497.2
Std.	118.3	78.5	4.8	2.4	77.0	38.2	126.0	75.1	70.4	26.8
CV	0.31	0.19	0.05	0.02	0.22	0.09	0.31	0.11	0.18	0.05

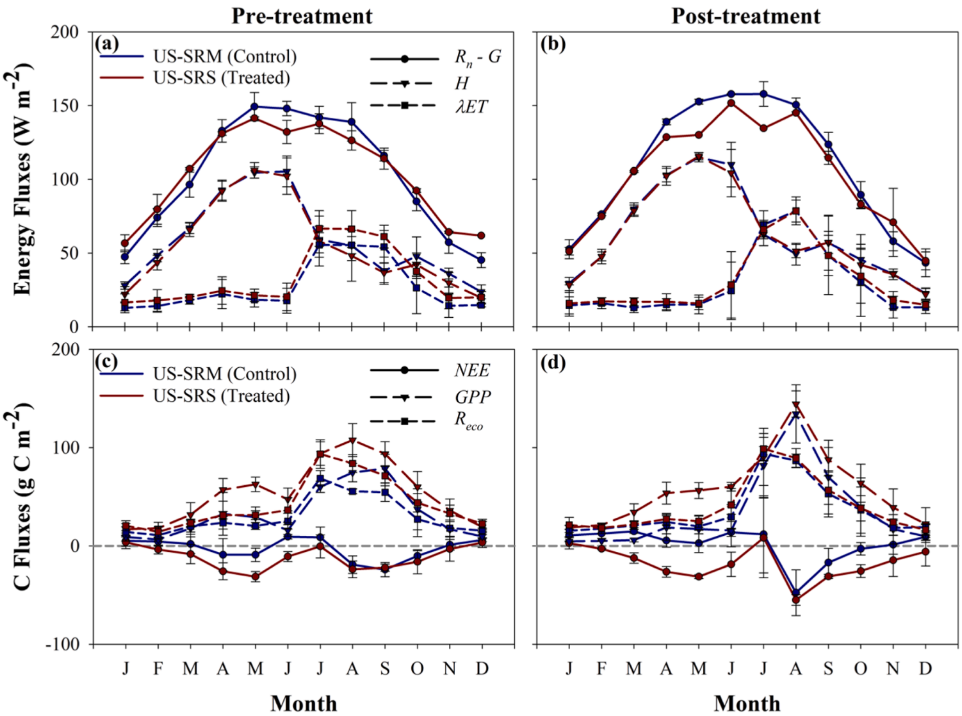

Fig. 5. Monthly water, energy, and carbon fluxes at US-SRM and US-SRS sites for pre-treatment (left; 2012–2016) and post-treatment (right; 2016–2018): (a and b) available energy (R_n - G), sensible heat flux (H), and latent heat flux (λET), all in W m^{-2}; and (c and d) net ecosystem exchange (NEE), gross primary productivity (GPP), and ecosystem respiration (R_{eco}), all in g C m^{-2}. Bars represent ±1 monthly standard deviation. The treatment month (June 2016) is excluded. Table 5 presents statistical summaries.

Table 5
Mean (±1 standard deviation) seasonal and annual comparison of pre- and post-treatment periods at US-SRM and US-SRS for latent heat flux (λET, W m^{-2}), sensible heat flux (H, W m^{-2}), net ecosystem exchange (NEE, g C m^{-2}), gross primary productivity (GPP, g C m^{-2}), and ecosystem respiration (R_{eco}, g C m^{-2}). Data for AMJ in 2016 is omitted since it spans the herbicide application date. Bold indicates significant differences between pre- and post-treatment within each site; italics indicate significant differences between US-SRM and US-SRS (Mann-Whitney Rank Sum Tests; $p < 0.05$). Seasons denoted as JFM (January – March), AMJ (April – June), JAS (July – September), and OND (October – December). Rank distribution tests of the median, 25%, and 75% quartiles are applied to pre- and post-treatment groups since these have different samples sizes (N_{pre} = 1461 days, N_{post} = 730 days) and failed the Shapiro-Wilk Normality Test.

Site	JFM		AMJ		JAS		OND		Annual	
	Pre-	Post-	Pre-	Post-	Pre-	Post-	Pre-	Post-	Pre-	Post-
US-SRM (control)										
λET	15±2	15±1	18±6	18±10	55±3	66±15	19±7	19±11	27±4	29±12
H	48±3	53±3	102±5	109±8	51±2	56±11	36±6	35±6	59±2	64±8
NEE	12±14	38±3	−1 ± 17	22±20	−35±9	−53±76	−3 ± 11	8 ± 18	−23±23	25±142
GPP	33±11	16±1	67±26	52±43	213±10	286±99	64±30	66±47	374±66	403±235
R_{eco}	45±13	54±5	66±15	74±23	179±7	234±23	61±24	74±32	351±49	428±93
US-SRS (treated)										
λET	18±4	17±1	21±7	20±11	65±5	65±4	26±2	23±8	33±2	31±6
H	44±4	52±1	100±7	108±8	48±8	57±3	31±2	33±5	55±2	62±5
NEE	−8 ± 16	−13±0	−65±17	−76±5	−46±12	−78±42	−16±26	−46±37	−133±44	−213±94
GPP	67±19	74±13	163±29	170±24	295±12	323±41	115±22	125±54	638±65	685±122
R_{eco}	58±11	62±12	98±20	94±29	249±18	245±17	99±13	79±19	505±23	472±28

the well-drained alluvial deposits surrounding the US-SRM site support more and larger shrubs than the poorly drained fan terrace at US-SRS. Higher water holding capacity of the clay subsoils at US-SRS also served to promote perennial grass cover, including a significant fraction of nonnative *Eragrostis* spp. that were largely absent at US-SRM. In addition, historical site disturbances have played a role in the differential mesquite shrub cover since US-SRS experienced both wildfire and brush management in the last 50 years. Furthermore, differences among the estimation methods for mesquite cover were small (<3%) for similar sampling years, indicating a robust set of image classifications for woody plants. The higher shrub cover at US-SRM (~28% over all dates and methods) relative to US-SRS (~17%) implies that a greater proportion of its satellite-based EVI would be attributable to mesquite shrubs which have been shown to follow the seasonal patterns illustrated here at other nearby sites (e.g., Scott et al., 2015; Perez-Ruiz et al., 2021).

Notable differences, however, were found among the grass and bare soil cover estimates based on the transect sampling and the NAIP classifications. Overall, this is attributed to offsets in the data collection times for the methods since both grass and bare soil cover are temporally dynamic. In addition, NAIP classifications were potentially subject to uncertainties related to grass patch size, color relative to bare soil, and obstruction of soil and grass cover underneath mesquite shrub canopies. For example, NAIP generally showed lower grass cover at US-SRM (~39% over all dates and methods) than at US-SRS (~49%), but similar amounts of bare soil cover (~33% and ~34% at US-SRM and US-SRS, respectively). Lower mesquite shrub cover at US-SRS was associated with higher grass cover, such that a greater proportion of EVI at the treated site was due to grass contributions. Since spring and summer EVI was greater at the US-SRM site throughout the study period, mesquite phenology was considered to be the dominant component in the satellite-based product. As a result, EVI products from MODIS do not readily provide a means for quantifying the relative contribution of grass cover at US-SRS to vegetation dynamics. Comparisons to MODIS EVI at a nearby grassland with only 11% mesquite shrub cover (Scott et al.,

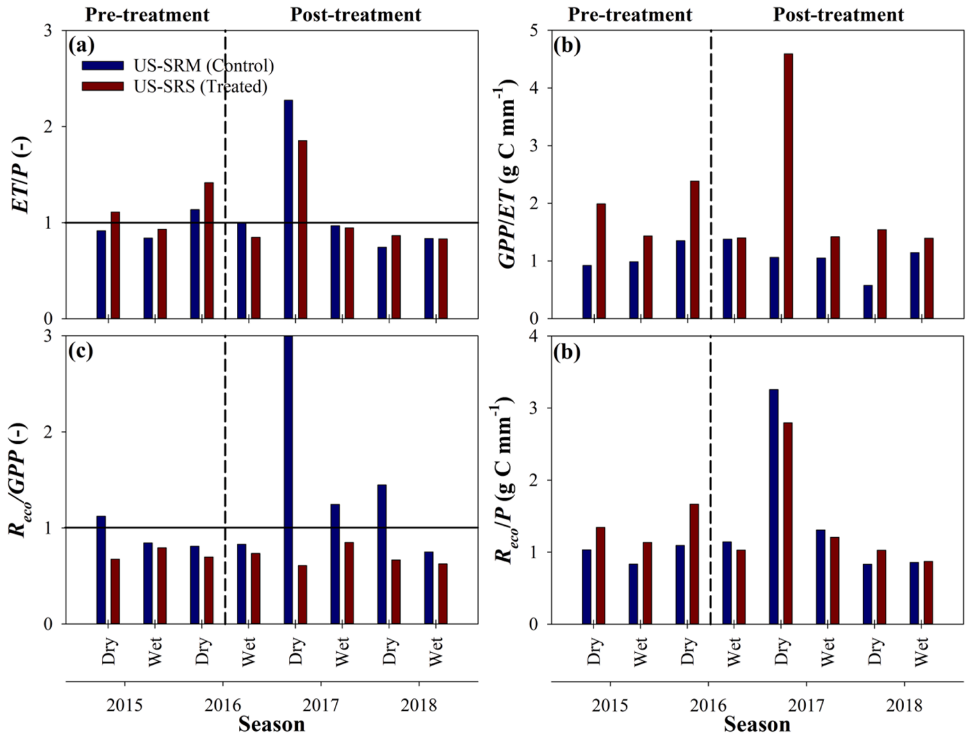

Fig. 6. Seasonal ratios of (a) ET/P, (b) water use efficiency (GPP/ET), (c) R_{eco}/GPP, and (d) R_{eco}/P at the US-SRM and US-SRS sites prior to and after the herbicide application. Dry and wet seasons refer to the period before (January to June) and after the North American monsoon (July to December), respectively. Vertical dashed lines depict the treatment date.

2015) revealed that perennial grasses show higher spring and summer *EVI* values (0.02 to 0.05 units greater, respectively) than at US-SRM and US-SRS. To improve the distinction between grass and bare soil cover and to capture the effect of grasses on the site phenology would require imagery at higher spatio-temporal resolutions, for instance from unmanned systems (e.g., Vivoni et al., 2014; Cunliffe et al., 2016).

5.2. Herbicide effect on vegetation and micrometeorological fluxes

Mesquite shrubs (*Prosopis* spp.) are highly tolerant of disturbance and are known to rebound quickly after brush management treatments (Bovey, 2016). The herbicide application, which consisted of a chemical formulation widely used by rangeland managers in the region (e.g., Ansley et al., 2004; Saleh et al., 2009), had a negligible impact on mesquite survival and only a small, transient effect on mesquite cover. Mesquite foliar loss was, however, significant during the first two months following herbicide application and had a measurable impact on *EVI* (e.g., ~0.5-unit reduction, green-up delay of ~1 month, and relative absence of seed pod formation). *EVI* at the US-SRS site recovered during the NAM season in response to herbaceous greenup, while mesquite foliar cover increased until reaching nearly undisturbed levels within two years, except for some crown tops. In response to the treatment, US-SRS exhibited large changes in grass and bare soil cover that were absent at US-SRM. Image classifications in the post-treatment period indicated a decrease in grass cover accompanied by an increase in bare soil for dates prior to the NAM. The unexpected reduction of perennial grass cover and associated expansion of bare soil cover could have favored mesquite recovery because of reduced competition and leading to more resiliency to the herbicide treatment. Deviations from anticipated grass recovery shortly (1 to 2 yr) after mesquite treatment were also noted by Ansley et al. (2021). Grass cover reduction, however, might be short-lived, as Herbel et al. (1983) and McClaran and Angell (2006) have shown that treatments can increase grass cover over decadal time frames.

Since meteorological conditions on the control and treated sites did not vary significantly during the post-treatment period, we attributed flux differences at the US-SRS site to vegetation attributes, wherein the lack of herbicide-induced shrub mortality or stem 'top-kill' and the rapid re-establishment of shrub foliar cover played a more important role than direct or indirect treatment effects on grass productivity. A decrease in R_n in the cool season after treatment was a direct result of lower mesquite shrub and grass cover accompanied by an expansion of exposed soils. Similarly, a temporary reduction in λET and a small increase in H occurred at the US-SRS site, relative to the US-SRM site, for the NAM season and the subsequent cool season. Herbicide-induced vegetation changes resulted in a reversal of the relative amounts of ET/P and R_{eco}/P at the two sites. Prior to treatment, US-SRS had higher ET/P throughout the year. However, the reduction in both mesquite foliage and grass cover promoted a lower ET/P, relative to the US-SRM site, which was linked to reduced plant uptake of deep soil water in the dry season and of shallow soil water use in the wet season (Scott and Biederman, 2019). This suggests the herbicide treatment modestly impacted the ET/P ratio for at least two years.

Mesquite foliar dynamics on the treated site played an important role in altering the carbon fluxes. While ET/P was suppressed at US-SRS relative to the US-SRM site, sustained amounts of ET and GPP resulted in relatively more CO_2 uptake at the US-SRS site for the subsequent spring and summer after the treatment. Initially, US-SRS had a relative reduction in water use efficiency. However, GPP/ET increased substantially in the spring as mesquite shrubs leafed-out taking advantage of deep soil water and potentially less competition from perennial grasses. Differences between GPP/ET at US-SRS and US-SRM diminished after one year. Net CO_2 uptake at the US-SRS site was also influenced by a reversal in the relative magnitude of R_{eco}/P among sites which lasted at least two years. R_{eco}/GPP remained low at US-SRS after the treatment, despite a period of higher values at the US-SRM site. The lower amounts of CO_2 released back to the atmosphere at US-SRS were attributed to the expansion of bare soil cover and reductions of perennial grass cover. Along with differences in water fluxes relative to the US-SRM site, these results suggest that the herbicide treatment temporarily reorganized the carbon flux magnitudes leading to more net CO_2 uptake during recovery.

5.3. Limitations in micrometeorological flux comparisons

The effect of herbicide treatment was discerned through comparisons between two sites for several years prior to and after the aerial application. This allowed for a detailed assessment that accounts for pre-treatment differences in micrometeorological conditions linked to soil type, vegetation composition, disturbance history, and measurement discrepancies. As such, the outcomes were determined through assessing changes at the US-SRS site relative to those at the US-SRM site. Measurement differences associated with the instrumentation and their setup on the two sites may have impacted comparisons to some extent. As noted previously, minor setup variations were present (e.g., sensor height variation of 1 m, sensor orientation difference of 15°, and sampling frequencies of 10 and 20 Hz). While we performed similar data processing steps and quality control measures consistent with AmeriFlux standards (Novick et al., 2018), recent studies have shown that eddy covariance instruments (specifically, the open-path infrared gas analyzer) themselves can have biases associated with sensor differences for the same manufacturer model (e.g., Scott et al., 2015; Deventer et al., 2020). As a result, we caution against site comparisons in absolute terms within the pre- and post-treatment periods and recommend collection of both pre- and post-treatment data whenever possible. Here, pre-treatment characterizations support interpretations of herbicide-induced changes based upon relative and normalized flux measures, despite the above-mentioned sensor differences. Without the pre-treatment observations and analyses, it would not have been possible to: (1) quantify the relative changes in vegetation and bare soil cover which illustrated an unexpected decrease in perennial grasses at the treated site, (2) characterize which changes in the post-treatment period were due to meteorological differences with the pre-treatment period or due to vegetation changes induced by the herbicide application, and (3) detect the reversal in the relative magnitudes of the water and carbon indices (ET/P, R_{eco}/P) among the two sites which are considered to be an important signature of the effect of the herbicide application. Most brush management studies rarely account for site differences that might occur prior to treatment. In drylands characterized by substantial heterogeneities in soils, vegetation, and disturbance histories, the implicit assumption of similar site characteristics prior to treatment should be evaluated before interpreting the effectiveness of a brush management strategy.

6. Conclusions

This study explored the effects of an aerially-applied herbicide on vegetation structure and micrometeorological fluxes in a semiarid savanna through a direct comparison to a nearby untreated area of similar characteristics. In the Sonoran Desert, mesquite shrubs have encroached upon perennial grasslands leading to dramatic, long-term changes in ecosystem structure and processes (e.g., Archer et al., 2017). While reversing these impacts through different brush management practices is attractive to rangeland managers in the region, there is a paucity of studies that have quantified their effectiveness from the perspective of impacts on micrometeorological fluxes. For instance, Huang et al. (2020) describe how brush management in sparse semiarid biomes can often result in unanticipated outcomes when based on paradigms developed in more mesic ecosystems. In this study, we conducted a quantitative evaluation of herbicide-induced changes in a Sonoran Desert mesquite savanna, an ecosystem with counterparts in the Chihuahuan Desert and Southern Great Plains. We focused on ascertaining how an herbicide application, a common rangeland management practice, would affect water, energy, and carbon fluxes as measured by the eddy covariance method.

The herbicide treatment defoliated the majority of the mesquite shrubs leading to a temporary reduction in summer greening relative to the control site. Unexpectedly, perennial grasses decreased and bare soil increased in cover at the treatment site during the mesquite recovery. There was negligible mesquite mortality and the herbicide effects on mesquite foliar cover lasted less than two years, during which time mesquite shrubs continued to exploit deep soil water sources. Thus, from the perspective of brush management, the herbicide application was not effective. From an ecological perspective, the herbicide-induced disturbance temporarily impacted micrometeorological fluxes, showing the effect of single treatment on mesquite shrubs. Relative comparisons revealed that changes in the vegetation structure, not site variations in microclimate conditions, topoedaphic factors, and historical land use, were the main drivers of the flux differences on the treated and control sites. Mesquite foliar loss led to changes in the relative site magnitudes of water and carbon indices with recovery to pre-treatment levels after at least two years. During mesquite recovery, net CO_2 uptake was enhanced through a combination of higher relative gross primary productivity and a relative decrease in ecosystem respiration. Perennial grasses are known to influence mesquite performance (Simmons et al., 2007; Holdo and Brocato, 2015). Accordingly, reductions in perennial grass cover during the post-treatment period may have relaxed grass-on-shrub competition and played a role in the observed mesquite-driven micrometeorological flux differences. Given the limited treatment effectiveness observed, the need for follow-up brush management treatments should be factored into long-term planning (e.g., Fulbright, 1996; Teague et al., 2001; Archer et al., 2011). This data suggests that the timing of such follow-up applications should target the subsequent spring season during periods when mesquite allocation to belowground structures is likely occurring. According to the micrometeorological fluxes observed in this study, this phenological timing could be indicated by periods of high water use efficiency in the spring season before shrubs have had a chance to fully recoup reserves expended after treatment the prior growing season (e.g., Noble et al., 2001).

Declaration of Competing Interest

The authors declare that they have no known competing financial interests or personal relationships that could have appeared to influence the work reported in this paper.

Acknowledgement

We acknowledge funding from the U.S. Department of Agriculture (2015-67019-23314), U.S. Army Research Office (56059-EV-PCS), the Department of Energy's Office of Science (for US-SRM operations) and Arizona Agricultural Experiment Station (ARZT-1361610-H12-223). We thank Ross Bryant, Adam P. Schreiner-McGraw, and Cody A. Anderson for help with equipment maintenance and data collection. The USDA is an EEO employer. Datasets for US-SRM and US-SRS are available from the AmeriFlux network, which is funded by the U.S. Department of Energy's Office of Science. Undergraduates Alyiah Branz, Cameron Burleson, Victoria Friess, Ethan Finch, Alex Grant, Travis McElroy, Alaina Michaels, Kalyn Miller, Jesus Quinn, Courtney Pijanowski, Sarah Posner, Damian Radine, Emily Runnion, Carley Schwartz, Alyssa Sierra, Bridget Slomka, and Karen Wang provided field vegetation data collection support. Thoughtful comments and suggestions from two anonymous reviewers helped improve the manuscript. Data sets are available at: (1) US-SRM at http://ameriflux.lbl.gov/sites/siteinfo/US-SRM, and (2) US-SRS at http://ameriflux.lbl.gov/sites/siteinfo/US-SRS.

References

Alfieri, J.G., Blanken, P.D., 2012. How representative is a point? The spatial variability of surface energy fluxes across short distances in a sand-sagebrush ecosystem. J. Arid Environ. 87, 42–49.

Anderson, C.A., Vivoni, E.R., 2016. Land surface states within the flux footprint impact land-atmosphere coupling in two semiarid ecosystems of the southwestern U.S. Water Resour. Res 52, 4785–4800.
Ansley, R.J., Pinchak, W.E., Teague, W.R., Kramp, B.A., Jones, D.L., Jacoby, P.W., 2004. Long-term grass yields following chemical control of honey mesquite. J. Rangeland Manage. 57, 49–57.
Ansley, R.J., Steffens, T.J., Cooper-Norris, C.E., Zhang, T., 2021. Herbaceous production and soil nitrogen after mesquite mortality in Southern Great Plains (US) grassland. Rangeland Ecol. Manage. 77, 82–92.
Pages 105-170 Archer, S., Davies, K., Fulbright, T., McDaniel, K., Wilcox, B., Predick, K. I., 2011. Brush management as a rangeland conservation strategy: a critical evaluation. In: Briske, D. (Ed.), Conservation Benefits of Rangeland practices: Assessment, recommendations, and Knowledge Gaps. United States Department of Agriculture, Natural Resources Conservation Service, Washington, DC.
Pages 25–84 Archer, S., Andersen, E., Predick, K.I., Schwinning, S., Steidl, R., Woods, S., 2017. Woody plant encroachment: causes and consequences. In: Briske, D. (Ed.), Rangeland Systems: Processes, Management and Challenges. Springer Series on Environmental Management. https://doi.org/10.1007/978-3-319-46709-2_2.
Archer, S., Predick, K.I., 2014. An ecosystem services perspective on brush management: research priorities for competing land-use objectives. J. Ecol. 102, 1394–1407. https://doi.org/10.1111/1365-2745.12314.
Baldocchi, D., Hicks, B.B., Meyers, T.P., 1988. Measuring biosphere-atmosphere exchanges of biologically related gases with micrometeorological method. Ecology 69, 1331–1340.
Biederman, J.A., Scott, R.L., Goulden, M.L., Vargas, R., Litvak, M.E., Kolb, T.E., Yepez, E. A., Oechel, W.C., Blanken, P.D., Bell, T.W., Garatuza-Payan, J., Maurer, G.E., Dore, S., Burns, S.P., 2016. Terrestrial carbon balance in a drier world: the effects of water availability in southwestern North America. Glob. Change Biol 22 (5), 1867–1879.
Biederman, J.A., Scott, R.L., Arnone, J., Jasoni, R.L., Litvak, M.E., Moreo, M.T., Papuga, S.A., Ponce-Campos, G.E., Schreiner-McGraw, A.P., Vivoni, E.R., 2018. Shrubland carbon sink depends upon winter water availability in the warm deserts of North America. Agric. For. Meteorol. 249, 407–419.
Beck, H.E., Zimmermann, N.E., McVicar, T.R., Vergopolan, N., Berg, A., Wood, E.F., 2018. Present and future Koppen-Geiger climate classification at 1-km resolution. Sci. Data 5, 180214. https://doi.org/10.1038/sdata.2018.214.
Bovey, R.W., 2016. Mesquite: History, Growth, Biology, Uses, and Management. Texas A&M University Press, p. 280.
Breckenfeld, D.J., Robinett, D., 2003. Soil and ecological sites of the Santa Rita Experimental Range. A Century of Vegetation Change on the Santa Rita Experimental Range, in Santa Rita Experimental Range: 100 Years (1903 to 2003) of Accomplishments and Contributions. U.S. Department of Agriculture, Forest Service, Rocky Mountain Research Station, Tucson, AZ, pp. 157–165.
Browning, D., Archer, S., Asner, G., McClaran, M., Wessman, C., 2008. Woody plants in grasslands: post-encroachment stand dynamics. Ecol. Appl. 18, 928–944.
Cable, D.R., 1975. Influence of precipitation on perennial grass production in the semidesert southwest. Ecology 56, 981–986. https://doi.org/10.2307/1936309.
Cable, D.R., 1977. Seasonal use of soil water by mature velvet mesquite. J. Range Manage. 30, 4–11. https://doi.org/10.2307/3898220.
Chen, X., Hutley, L.B., Eamus, D., 2003. Carbon balance of a tropical savanna of northern Australia. Oecologia 137, 405–416.
Chu, H., Luo, X., Ouyang, Z., Chan, W.S., Dengel, S., Biraud, S.C., Torn, M.S., Metzger, S., Kumar, J., Arain, M.A., Arkebauer, T.J., Balocchi, D., Bernacchi, C., Billesbach, D., Black, T.A., Blanken, P.D., Bohrer, G., Bracho, R., Brown, S., Brunsell, N.A., Chen, J., Chen, X., Clark, K., Desai, A.R., Duman, T., Durden, D., Fares, S., Forbrich, I., Gamon, J.A., Gough, C.M., Griffis, T., Helbig, M., Hollinger, D., Humphreys, E., Ikawa, H., Iwata, H., Ju, Y., Knowles, J.F., Knox, S.H., Kobayashi, H., Kolb, T., Law, B., Lee, X., Litvak, M., Liu, H., Munger, J.W., Noormets, A., Novick, K., Oberbauer, S.F., Oechel, W., Oikawa, P., Papuga, S.A., Pendall, E., Prajaya, P., Prueger, J., Quinton, W.L., Richardson, A.D., Russell, E.S., Scott, R.L., Starr, G., Staebler, R., Stoy, P.C., Stuart-Haentjens, E., Sonnentag, O., Sullivan, R.C., Suyker, A., Ueyama, M., Vargas, R., Wood, J.D., Zona, D., 2021. Representativeness of eddy-covariance flux footprints for areas surrounding AmeriFlux sites. Agric. For. Meteorol. 301-302, 108350. http://doi.org/10.1016/j.agrformet.2021.108350.
Cunliffe, A.M., Brazier, R.E., Anderson, K., 2016. Ultra-fine grain landscape-scale quantification of dryland vegetation structure with drone-acquired structure-from-motion photogrammetry. Remote Sens. Environ. 183, 129–143.
Detto, M., Montaldo, N., Albertson, J.D., Mancini, M., Katul, G., 2006. Soil moisture and vegetation controls on evapotranspiration in a heterogeneous Mediterranean ecosystem on Sardinia, Italy. Water Resour. Res. 42, W08419. https://doi.org/10.1029/2005WR004693.
Deventer, M.J., Roman, T., Bogoev, I., Kolka, R.K., Erickson, M., Lee, X., Baker, J.M., Millet, D.B., Griffis, T.J., 2020. Biases in open-path carbon dioxide flux measurements: roles of instrument surface heating exchange and analyzer temperature sensitivity. Agri. For. Meteorol. 296, 108216 https://doi.org/10.1016/j.agrformet.2020.108216.
Ding, J., Travers, S.K., Delgado-Baquerizo, M., Eldridge, D.J., 2020. Multiple trade-offs regulate the effects of woody plant removal on biodiversity and ecosystem functions in global rangelands. Glob. Change Biol 26 (2), 709–720.
Dugas, W.A., Hicks, R.A., Gibbens, R.P., 1996. Structure and function of C3 and C4 Chihuahuan Desert plant communities. Energy balance components. J. Arid Environ. 34 (1), 63–79. https://doi.org/10.1006/jare.1996.0093.
El-Madany, T.S., Reichstein, M., Perez-Priego, O., Carrara, A., Moreno, G., Martin, M.P., Pacheco-Labrador, J., Wohlfahrt, G., Nieto, H., Weber, U., Kolle, O., Luo, Y.-P., Carvalhais, N., Miglivaca, M., 2018. Drivers of spatio-temporal variability of carbon dioxide and energy fluxes in a Mediterranean savanna ecosystem. Agri. For. Meteorol. 262, 258–278.
Field, C.B., Behrenfeld, M.J., Randerson, J.T., Falkowski, P., 1998. Primary production of the biosphere: integrating terrestrial and oceanic components. Science 281, 237–240.
Falge, E., Baldocchi, D., Olson, R., Anthoni, P., Aubinet, M., Bernhofer, C., Burba, G., 2001. Gap Filling Strategies for Defensible Annual Sums of Net Ecosystem Exchange. Agricultural and Forest Meteorology 107 (1), 43–69. https://doi.org/10.1016/S0168-1923(00)00225-2.
Fulbright, T.E., 1996. Viewpoint: a theoretical basis for planning woody plant control to maintain species diversity. J. Range Manage. 49, 554–559.
Goodrich, D.C., Keefer, T.O., Unkrich, C.L., Nichols, M.H., Osborn, H.B., Stone, J.J., Smith, J.R., 2008. Long-term precipitation database, Walnut Gulch Experimental Watershed, Arizona, United States. Water Resour. Res. 44, W05S04. https://doi.org/10.1029/2006WR005782.
Hamilton, W.T., McGinty, A., Ueckert, D.N., Hanselka, C.W., Lee, M.R., 2004. Brush Management: Past, Present, Future. Texas A&M University Press, College Station, TX, p. 296.
Herbel, C.H., Gould, W.L., Leifeste, W.F., Gibbens, R.P., 1983. Herbicide treatment and vegetation response to treatment of mesquites in southern New Mexico. J. Range Manage. 36 (2), 149–151.
Hinojo-Hinojo, C., Castellanos, A.E., Huxman, T., Rodriguez, J.C., Vargas, R., Romo-Leon, J.R., Biederman, J.A., 2019. Native shrubland and managed buffelgrass savanna in drylands: implications for ecosystem carbon and water fluxes. Agri. For. Meteorol. 268, 269–278.
Holdo, R.M., Brocato, E.R., 2015. Tree-grass competition varies across select savanna tree species: a potential role for rooting depth. Plant Ecol. 216, 577–588.
Huntington, J., Hegewisch, K., Daudert, B., Morton, C., Abatzoglou, J., McEvoy, D., Erickson, T., 2017. Climate Engine: cloud computing of climate and remote sensing data for advanced natural resource monitoring and process understanding. Bull. Amer. Meteorol. Soc. 98 (11), 2397–2410.
Huxman, T.E., Wilcox, B.P., Breshears, D.D., Scott, R.L., Snyder, K.A., Small, E.E., Hultine, K., Pockman, W.T., Jackson, R.B., 2005. Ecohydrological implications of woody plant encroachment. Ecology 86 (2), 308–319.
Huang, C.Y., Marsh, S.E., McClaran, M.P., Archer, S.R., 2007a. Postfire stand structure in a semiarid savanna: cross-scale challenges estimating biomass. Ecol. Appl. 17 (7), 1899–1910.
Huang, C.-W., Krofcheck, D.J., Duman, T., Fox, A.M., Pockman, W.T., Lippit, C.D., McIntire, C.D., Litvak, M.E., 2020. Ecosystem-level energy and water budgets are resilient to canopy mortality in sparse semiarid biomes. J. Geophys. Res. 125, e2020JG005858 https://doi.org/10.1029/2020JG005858.
Kljun, N., Calanca, P., Rotach, M.W., Schmid, H.P., 2015. A simple two-dimensional parameterisation for Flux Footprint Prediction (FFP). Geosci. Model Develop. 8 (11), 3695–3713.
Ma, X., Huete, A., Moore, C., Cleverly, J., Hutley, L., Beringer, J., Leng, S., Xie, Z., Yu, Q., Eamus, D., 2020. Spatiotemporal partitioning of savanna plant functional type productivity along NATT. Remote Sens. Environ. 246, 111855.
Martin, S.C., Morton, H.L., 1993. Mesquite control increases grass density and reduces soil loss in southern Arizona. J. Range Manage. 46 (2), 170–175.
McClaran, M.P., Angell, D.L., 2006. Long-term vegetation response to mesquite removal in Desert Grassland. J. Arid Environ. 66, 686–697.
Mendez-Barroso, L.A., Vivoni, E.R., Watts, C.J., Rodriguez, J.C., 2009. Seasonal and interannual relation between precipitation, surface soil moisture and vegetation dynamics in the North American monsoon region. J. Hydrol. 377, 59–70.
Morillas, L., Pangle, R.E., Maurer, G.E., Pockman, W.T., McDowell, N., Huang, C.-W., Krofcheck, D.J., Fox, A.M., Sinsabaugh, R.L., Rahn, T.A., Litvak, M.E., 2017. Tree mortality decreases water availability and ecosystem resilience to drought in piñon-juniper woodlands in the southwestern U.S. J. Geophys. Res. 122, 3343–3361.
Naito, A.T., Cairns, D.M., 2011. Patterns and processes of global shrub expansion. Prog. Phys. Geog. 35 (4), 423–442.
Noble, J.C., Grice, A.C., Dobbie, M.J., Muller, W.J., Wood, J.T., 2001. Integrated shrub management in semi-arid woodlands of eastern Australia: effects of chemical defoliants applied after an initial disturbance. Rangeland J. 23, 224–258.
Noble, J.C., 1997. The Delicate and Noxious scrub: CSIRO Studies on Native Tree and Shrub Proliferation in the Semi-Arid Woodlands of Eastern Australia. CSIRO Wildlife and Ecology, Canberra, Australia, p. 137.
Novick, K.A., Biederman, J.A., Desai, A.R., Litvak, M.E., Moore, D.J.P., Scott, R.L., Torn, M.S., 2018. The AmeriFlux network: a coalition of the willing. Agric. For. Meteorol. 249, 444–456.
O'Connor, T.G., Puttick, J.R., Hoffman, M.T., 2014. Bush encroachment in southern Africa: changes and causes. African J. Range Forage Sci. 31, 67–88.
Perez-Ruiz, E.R., Vivoni, E.R., Yepez, E.A., Rodriguez, J.C., Gochis, D.J., Robles-Morua, A., Delgado-Balbuena, J., Adams, D.K., 2021. Landscape controls on water-energy-carbon fluxes across different ecosystems during the North American monsoon. J. Geophys. Res. Biogeosci. 126, e2020JG005809 https://doi.org/10.1029/2020JG005809.
Pierini, N.A., Vivoni, E.R., Robles-Morua, A., Scott, R.L., Nearing, M.A., 2014. Using observations and a distributed hydrologic model to explore runoff threshold processes linked with mesquite encroachment in the Sonoran Desert. Water Resour. Res. 50 (10), 8191–8215.
Pima Association of Governments, 2011. LiDAR Campaign (Pima County, AZ) Report of Survey. Sanborn Total Geospatial Solutions, p. 15.
Polyakov, V.O., Nearing, M.A., Nichols, M.H., Scott, R.L., Stone, J.J., McClaran, M.P., 2010. Long-term runoff and sediment yields from small semiarid watersheds in southern Arizona. Water Resour. Res. 46 (9), W09512. https://doi.org/10.1029/2009WR009001.

Reichstein, M., Falge, E., Baldocchi, D.D., Papale, D., Aubinet, M., Berbigier, P., Bernhofer, C., Buchmann, N., Gilmanov, T., Granier, A., Grünwald, T., Havránková, K., Ilvesniemi, H., Janous, D., Knohl, A., Laurila, T., Lohila, A., Loustau, D., Matteucci, G., Meyers, T., Miglietta, F., Ourcival, J.-M., Pumpanen, J., Rambal, S., Rotenberg, E., Sanz, M., Tenhunen, J., Seufert, G., Vaccari, F., Vesala, T., Yakir, D., Valentini, R., 2005. On the separation of net ecosystem exchange into assimilation and ecosystem respiration: review and improved algorithm. Glob. Change Biol 11, 1424–1439. https://doi.org/10.1111/j.1365-2486.2005.001002.x.

Sala, O.E., Yahdjian, L., Havstad, K., Aguiar, M.R., 2017. Rangeland ecosystem services: nature's supply and humans' demand. In: Briske, D. (Ed.), *Rangeland Systems*. Springer Series on Environmental Management. Springer, Cham. https://doi.org/10.1007/978-3-319-46709-2_14.

Saleh, A., Wu, H., Brown, C.S., Teagarden, F.M., McWilliams, S.M., Hauck, L.M., Millican, J.S., 2009. Effect of brush control on evapotranspiration in the North Concho River watershed using the eddy covariance technique. J. Soil Water Conserv. 64 (5), 336–349.

Pages 1–15 Sayre, N.F., 2003. Recognizing history in range ecology: 100 years of science and management on the Santa Rita Experimental Range. In: McClaran, M.P., Ffolliott, P., Edminster, C. (Eds.), Santa Rita Experimental Range: 100 Years (1903 to 2003) of Accomplishments and Contributions. U.S. Department of Agriculture, Forest Service, Rocky Mountain Research Station, Ogden, UT, Tucson, AZ. Proc. RMRS-P-30.

Schmid, H.P., Grimmond, C.S.B., Cropley, F., Offerle, B., Su, H.B., 2000. Measurements of CO_2 and energy fluxes over a mixed hardwood forest in the mid-western United States. Agric. For. Meteorol. 103 (4), 357–374.

Schreiner-McGraw, A.P., Vivoni, E.R., Ajami, H., Sala, O.E., Throop, H.L., Peters, D.P.C., 2020. Woody plant encroachment is expected to have a larger impact than climate change on dryland water budgets. Sci. Rep. 10, 8112.

Schreiner-McGraw, A.P., Vivoni, E.R., 2018. On the sensitivity of hillslope runoff and channel transmission losses in arid piedmont slopes. Water Resour. Res. 54 (7), 4498–4518.

Scifres, C.J., 1980. Brush Management: Principles and Practices For Texas and the Southwest. Texas A & M University Press, College Station, TX, p. 360.

Scott, R.L., Jenerette, G.D., Potts, D.L., Huxman, T.E., 2009. Effects of seasonal drought on net carbon dioxide exchange from a woody-plant-encroached semiarid grassland. J. Geophys. Res. 114, G04004. https://doi.org/10.1029/2008JG000900.

Scott, R.L., Biederman, J.A., Hamerlynck, E.P., Barron-Gafford, G., 2015. The carbon balance pivot point of southwestern U.S. semiarid ecosystems: insights from the 21st century drought. J. Geophys. Res. 120, 2612–2624.

Scott, R.L., Biederman, J.A., 2019. Critical zone water balance over thirteen years in a semiarid savanna. Water Resour. Res. 55, 574–588.

Silva, J.F., Zambrano, A., Farinas, M., 2001. Increase in the woody component of seasonal savannas under different fire regimes in Calabozo, Venezuela. J. Biogeogr. 28 (8), 977–983.

Simmons, M.T., Archer, S.R., Ansley, R.J., Teague, W.R., 2007. Grass effects on tree (*Prosopis glandulosa*) growth in a temperate savanna. J. Arid Environ. 69, 212–227.

Teague, W.R., Ansley, R.J., Kreuter, U.P., Pinchack, W.E., McGrann, J.M., 2001. Economics of managing mesquite in north Texas: a sensitivity analysis. J. Range Manage. 54 (5), 553–560.

van Leeuwen, W.J.D., Davison, J.E., Casady, G.M., Marsh, S.E., 2010. Phenological characterization of desert sky island vegetation communities with remote sensing and climate time series data. Remote Sens. 2, 388–415.

Venter, Z.S., Cramer, M.D., Hawkins, H.J., 2018. Drivers of woody plant encroachment over Africa. Nat. Comm. 9, 2272. https://doi.org/10.1038/s41467-018-04616-8.

Verduzco, V.S., Garatuza-Payan, J., Yepez, E.A., Watts, C.J., Rodriguez, J.C., Robles-Morua, A., Vivoni, E.R., 2015. Variations of net ecosystem production due to seasonal precipitation differences in a tropical dry forest of northwest Mexico. J. Geophys. Res. Biogeosci. 120 (10), 2081–2094.

Vivoni, E.R., Moreno, H.A., Mascaro, G., Rodriguez, J.C., Watts, C.J., Garatuza-Payan, J., Scott, R.L., 2008. Observed relation between evapotranspiration and soil moisture in the North American monsoon region. Geophys. Res. Lett. 35, L22403. http://doi.org/10.1029/2008GL036001.

Vivoni, E.R., Perez-Ruiz, E.R., Keller, Z.T., Escoto, E.A., Templeton, R.C., Templeton, N. P., Anderson, C.A., Schreiner-McGraw, A.P., Mendez-Barroso, L.A., Robles-Morua, A., Scott, R.L., Archer, S.R., Peters, D.P.C., 2021. Long-term research catchments to investigate shrub encroachment in the Sonoran and Chihuahuan Deserts: santa Rita and Jornada Experimental Ranges. Hydrol. Process. 35, e14031. http://doi.org/10.1002/hyp.14031.

Vivoni, E.R., Rango, A., Anderson, C.A., Pierini, N.A., Schreiner-McGraw, A.P., Saripalli, S., Laliberte, A.S., 2014. Ecohydrology with unmanned aerial vehicles. Ecosphere 5 (10). https://doi.org/10.1890/ES14-00217.1 art130.

Williams, C.A., Albertson, J.D., 2004. Soil moisture controls on canopy-scale water and carbon fluxes in an African savanna. Water Resour. Res. 40, W09302. https://doi.org/10.1029/2004WR003208.

Wilson, K., Goldstein, A., Falge, E., Aubinet, M., Baldocchi, D., Berbigier, P., Berhhofer, C., Ceulemans, R., Dolman, H., Field, C., Grelle, A., Ibrom, A., Law, B.E., Kowalski, A., Meyers, T., Moncrieff, J., Monson, R., Oechel, W., Tenhunen, J., Valentini, R., Verma, S., 2002. Energy balance closure at FLUXNET sites. Agr. For. Meteorol. 113 (1–4), 223–243.

Xu, K., Metzger, S., Desai, A.R., 2017. Upscaling tower-observed turbulent exchange at fine spatio-temporal resolution using environmental response functions. Agr. For. Meteorol. 232, 10–22.